Characterization of Inductively Coupled Plasma Time-of-Flight Mass Spectrometry in Combination with Collision/Reaction Cell Technology Insights from highly time-resolved measurements

Marcel Burger[1#*], Lyndsey Hendriks[1#], Jérôme Kaeslin[1#], Alexander Gundlach-Graham[1], Bodo Hattendorf[1] and Detlef Günther[1]

[1]Laboratory of Inorganic Chemistry, ETH Zürich, Vladimir-Prelog-Weg 1, CH-8093 Zürich, Switzerland

[#]these authors contributed equally
[*]corresponding author

Wednesday 17th October, 2018

A Supplementary Information

List of Figures

List of Tables

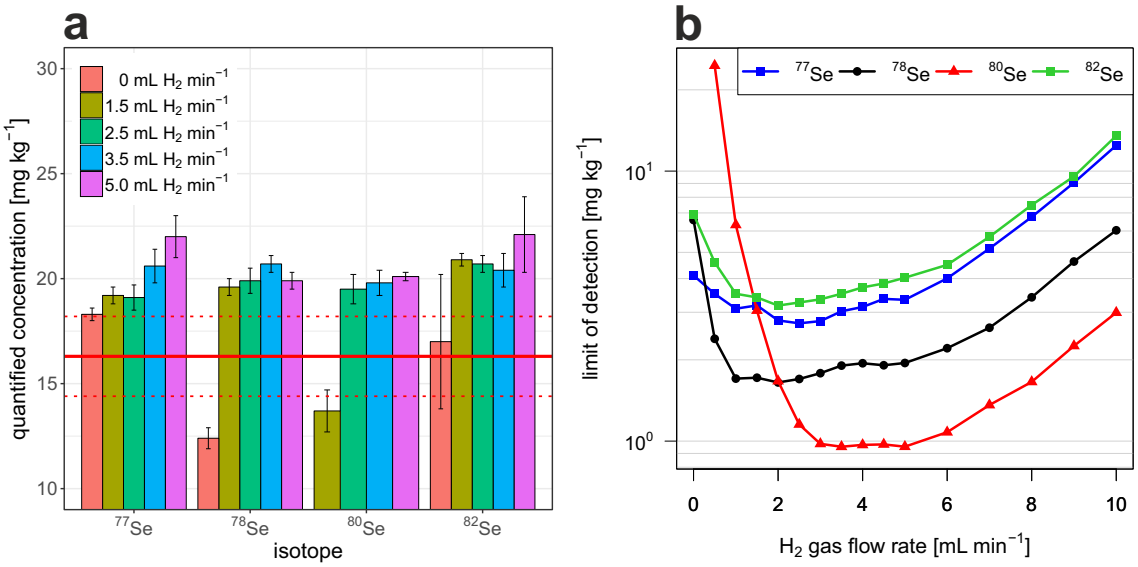

Figure A.1: Quantified Se concentration in NIST SRM 612 as a function of CCT conditions and isotope selection (a). Error bars represent the standard deviation calculated from three individual measurements. The solid red line represents the NIST SRM 612 reference concentration for Se reported in the GeoReM database.[1] The two dashed lines indicate the uncertainty range associated with the Se reference concentration. Limits of detection calculated for different Se isotopes as a function of H_2 gas flow rate through the reaction cell (b). Experiments were carried out using a 44 μm diameter circular spot and a laser repetition rate of 10 Hz. They were performed in line-scanning mode with a scan speed of 5 μm s^{-1}. NIST SRM 610 was used as external reference material. ^{29}Si was selected as the internal standard.

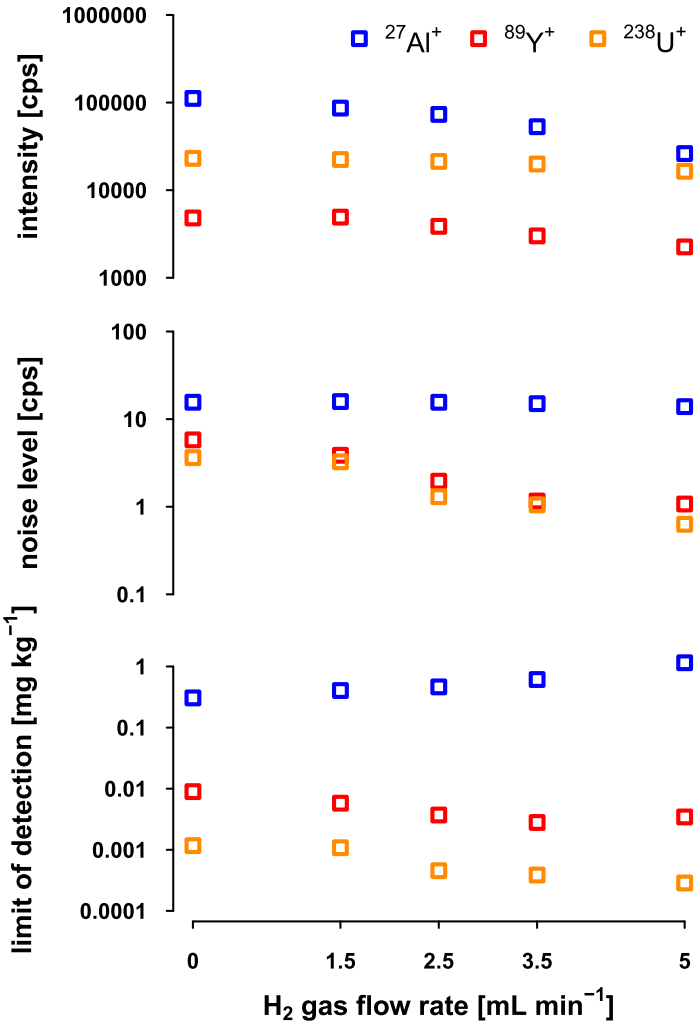

Figure A.2: Signal intensities, background noise levels (3σ) and calculated limits of detection as a function of the H_2 gas flow rate. Signal intensities were recorded during high-dispersion LA-ICP-CCT-TOFMS experiments carried out on NIST SRM 612 using a 44 μm diameter circular spot and a laser repetition rate of 10 Hz. The experiments were performed in line-scanning mode using a scan speed of 5 μm s^{-1}.

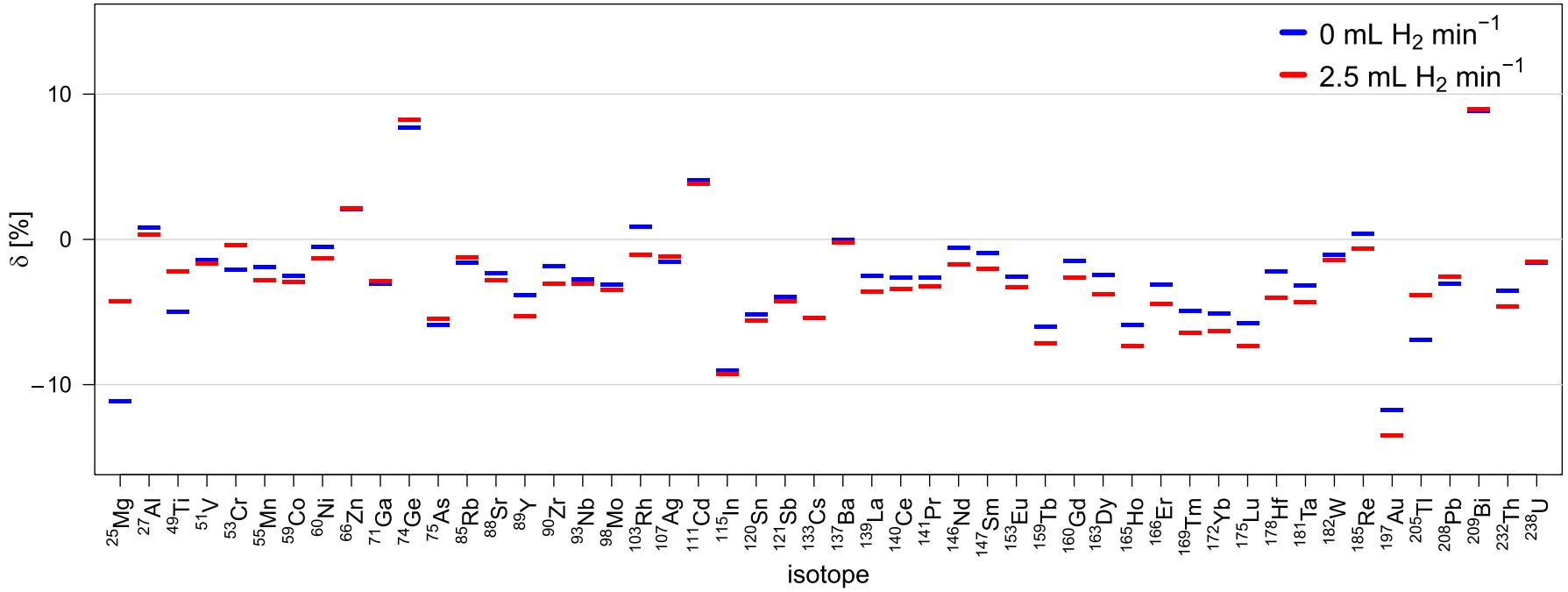

Figure A.3: Relative deviation of quantified element concentrations from NIST SRM 612 reference values reported in the GeoReM database.[1] Results are presented as a function of CCT conditions. Experiments were carried out using a 44 μm diameter circular spot and a laser repetition rate of 10 Hz. They were performed in line-scanning mode using a scan speed of 5 μm s^{-1}. NIST SRM 610 was used as external reference material. ^{27}Al was selected as the internal standard.

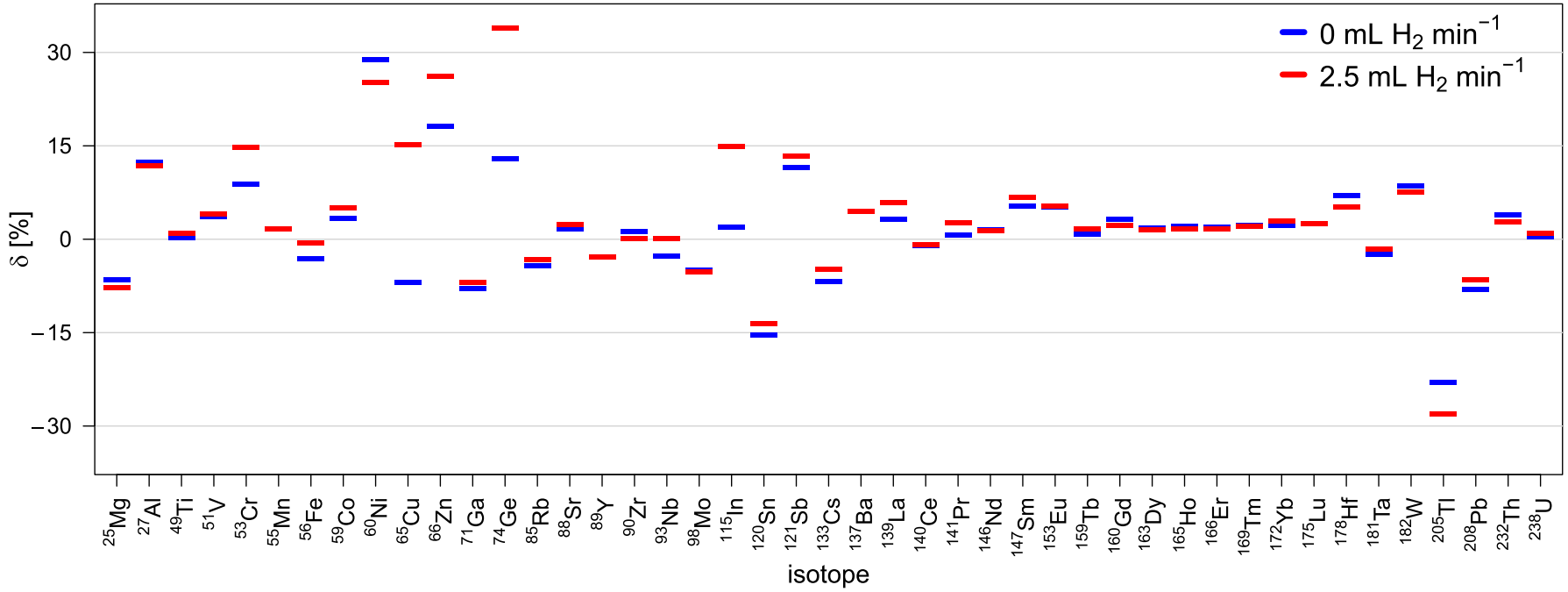

Figure A.4: Relative deviation of quantified element concentrations from USGS BCR-2G reference values reported in the GeoReM database.[1] Results are presented as a function of CCT conditions. Experiments were carried out using a 44 μm diameter circular spot and a laser repetition rate of 10 Hz. They were performed in line-scanning mode using a scan speed of 5 μm s^{-1}. NIST SRM 610 was used as external reference material. ^{29}Si was selected as the internal standard.

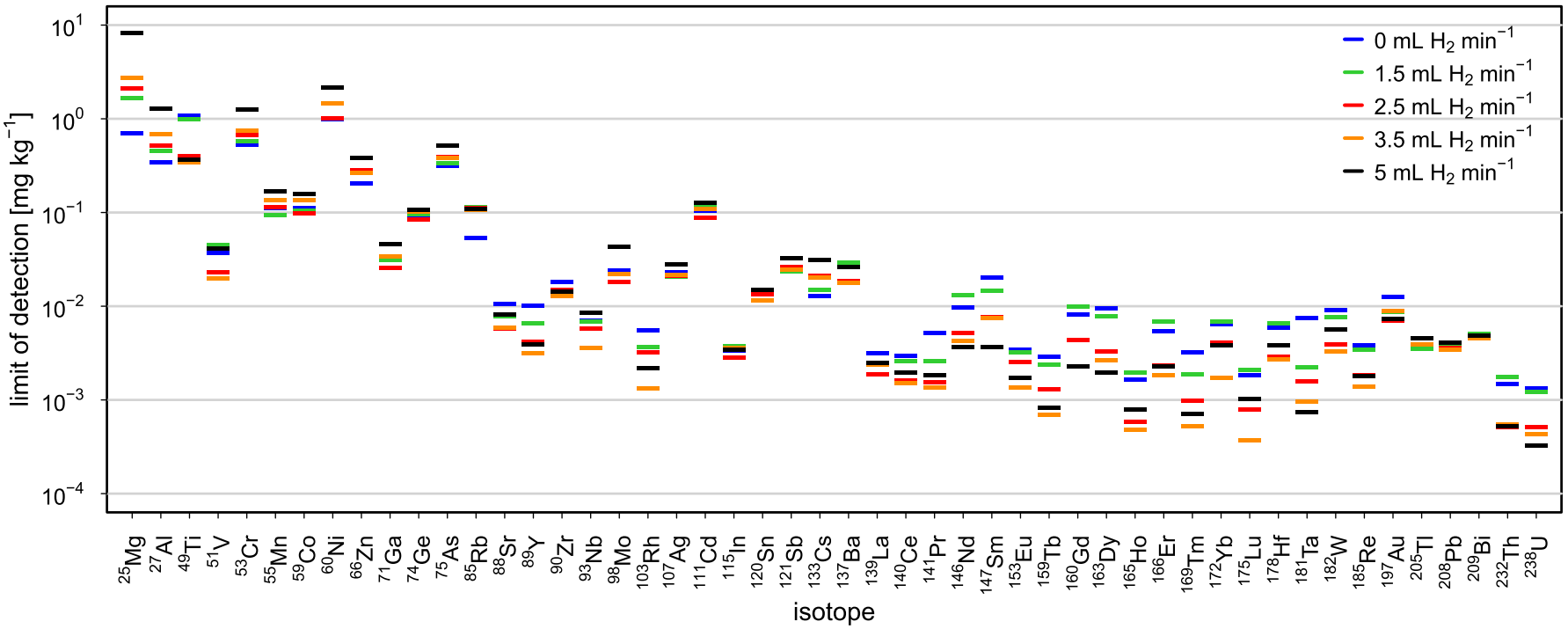

Figure A.5: Limits of detection as a function of CCT conditions. Experiments were carried out on NIST SRM 610 using a 44 μm diameter circular spot and a laser repetition rate of 10 Hz. They were performed in line-scanning mode using a scan speed of 5 μm s^{-1}.

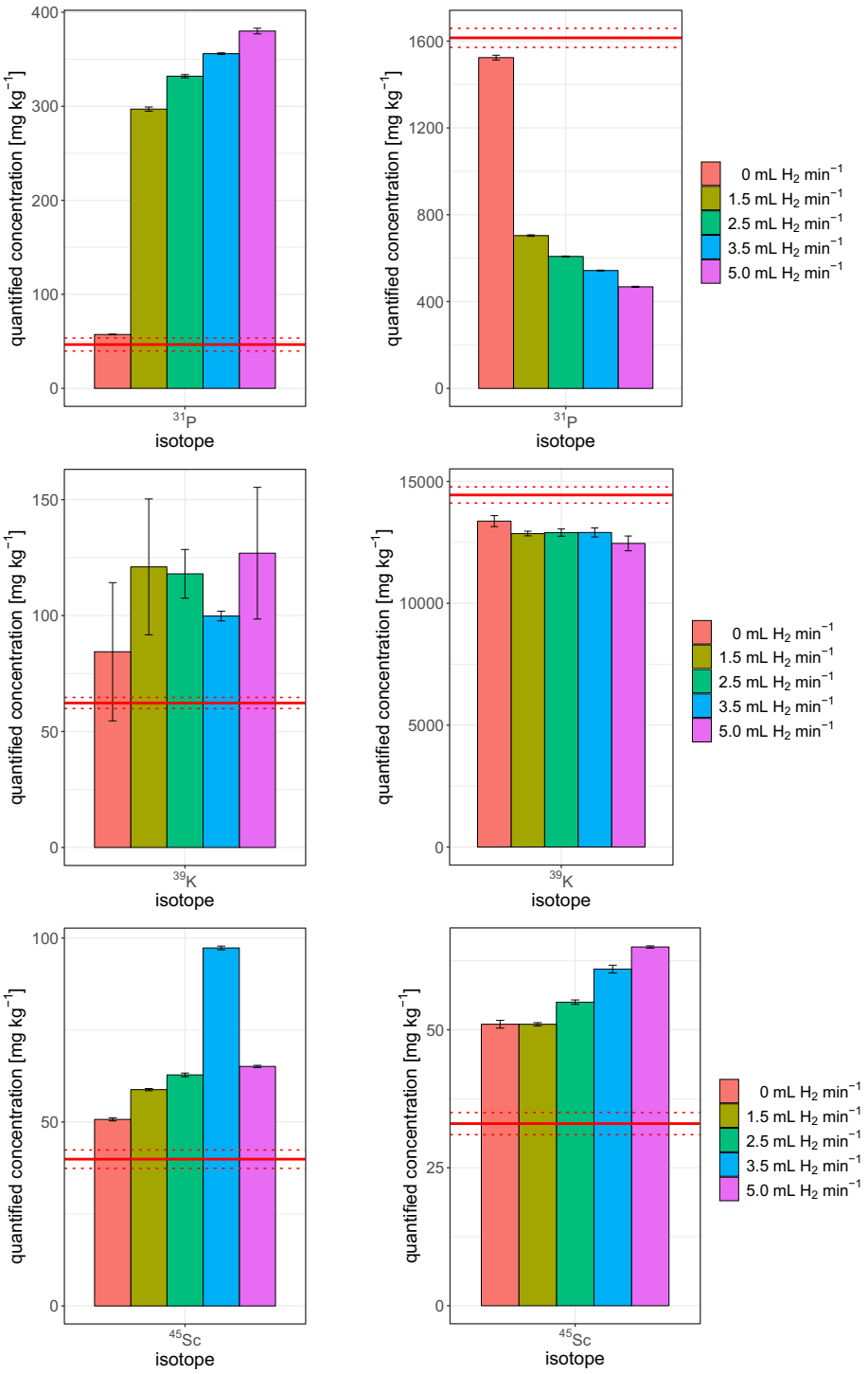

Figure A.6: Quantified Phosphorous, Potassium and Scandium concentration in NIST SRM 612 (left column) and USGS BCR-2G (right column) as a function of CCT conditions. Error bars represent the standard deviation calculated from three individual measurements. Experiments were carried out using a 44 μm diameter circular spot and a laser repetition rate of 10 Hz. They were performed in line-scanning mode with a scan speed of 5 μm s^{-1}. NIST SRM 610 was used as external reference material. ^{29}Si was selected as the internal standard. The solid red lines represent the NIST SRM 612 and USGS BCR-2G reference concentrations reported in the GeoReM database.[1] The two dashed lines indicate the uncertainty range associated with the reference concentrations.

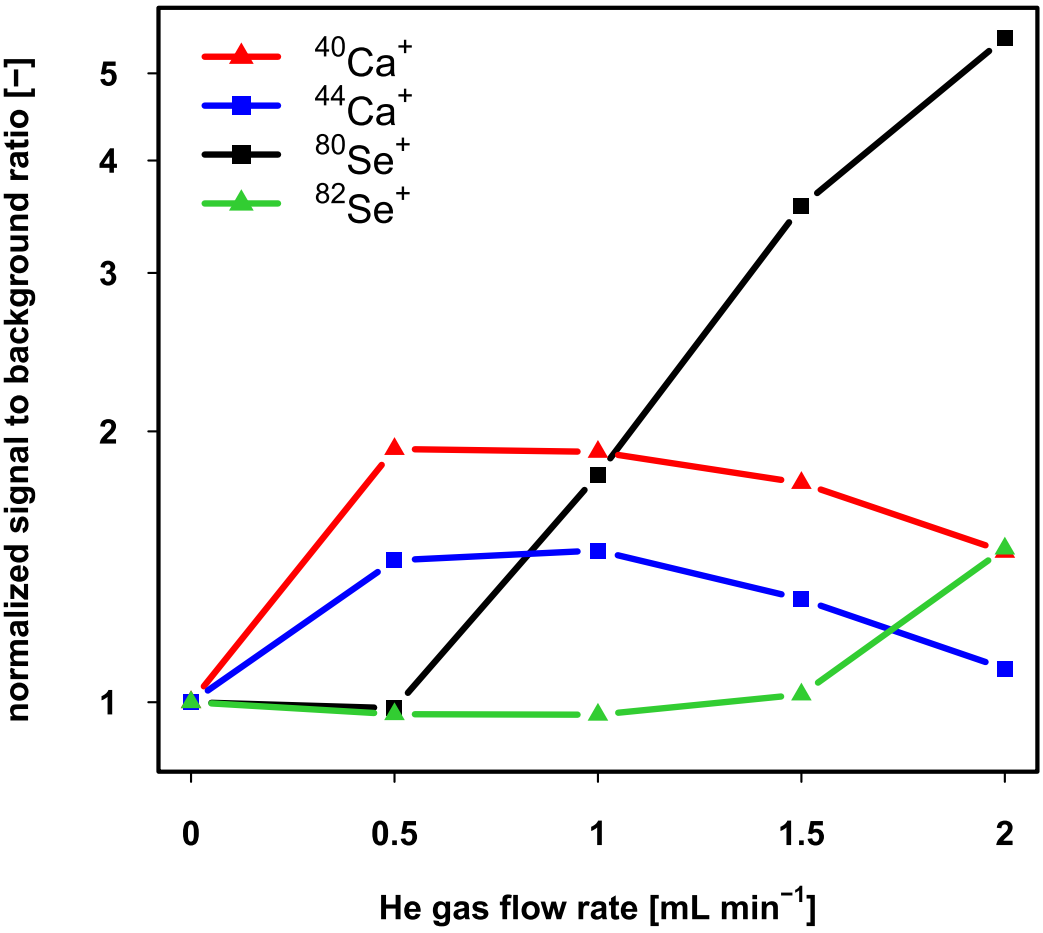

Figure A.7: Normalized signal to background ratios calculated for $^{40}Ca^{+}$, $^{44}Ca^{+}$, $^{80}Se^{+}$ and $^{82}Se^{+}$. Signal to background ratios reported here are normalized to the ones observed under standard conditions (no He gas addition). Data was acquired during a high-dispersion LA-ICP-CCT-TOFMS experiment as a function of the amount of He that was added to the constant H_2 gas flow rate of 1.5 mL min^{-1}. Experiments were carried out on NIST SRM 610 using a 44 μm diameter circular spot and a laser repetition rate of 10 Hz. They were performed in line-scanning mode using a scan speed of 5 μm s^{-1}. The multi-notch filter settings were kept constant at all times.

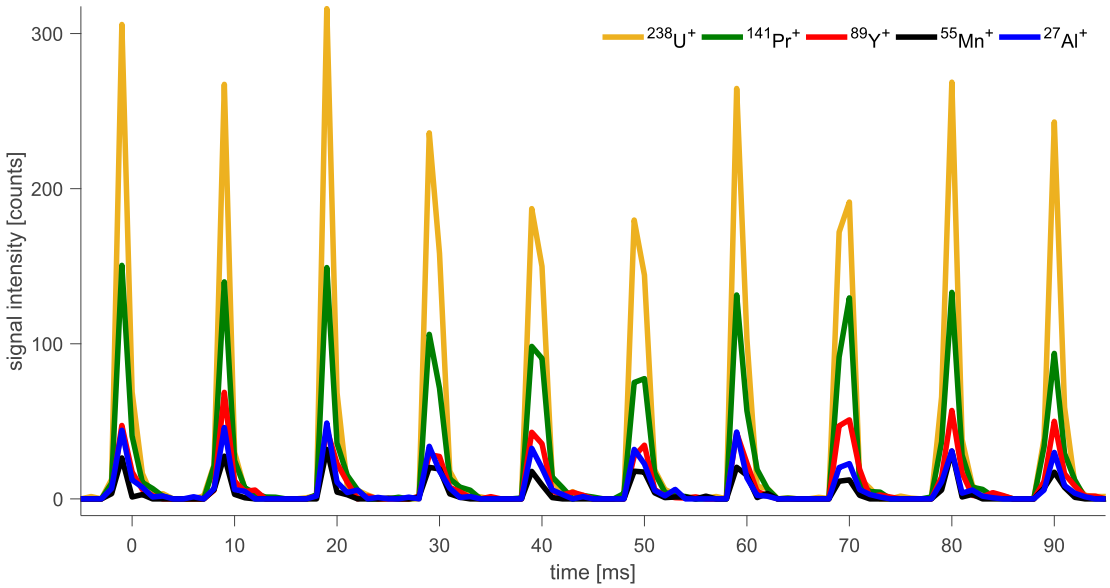

Figure A.8: Transient signal intensities recorded for selected isotopes during a low-dispersion LA-ICP-CCT-TOFMS experiment. Averaged elemental mass spectra were read out at a frequency of 1000 Hz. NIST SRM 610 was ablated using a 5 μm diameter circular spot and a laser repetition rate of 100 Hz. The experiment was carried out in line-scanning mode with a scan speed of 50 μm s^{-1}. In this study, a reaction gas flow rate of 2.5 mL H_2 min^{-1} was maintained. Similar results were also obtained with He as collision gas. Flow rates of up to 3.5 mL min^{-1} were tested.

Table A.1: Average signal intensities recorded for the entire elemental *m/z* range when analyzing gas-blank as a function of H_2 gas flow rate through the reaction cell. Time traces of 30 s duration were evaluated. The signal intensities and the associated uncertainties are the average value and the standard deviation calculated from analysis of 30 individual mass spectra. Mass spectra were baseline subtracted before signal intensities were integrated. Integration was done across mass windows with a width of one atomic mass unit. These mass windows were centered at the unit *m/z* indicated in the left column of Table A.1. Signal intensities are only reported in Table A.1 if their integrated intensity surpasses the Poisson critical level (CL) calculated using the signal intensity within the mass window centered at *m/z* 220 as a measure for non-specific noise. Species that account for or contribute to the signal intensities recorded within the respective mass windows are reported in the second column of the table and were determined by spectral evaluation taking into account a given specie's exact mass and natural isotopic abundances. No species is suggested when identification of the observed peak was not possible.

m/z	**species**	**intensity [cps] (0 mL H_2 min^{-1})**	**intensity [cps] (2.5 mL H_2 min^{-1})**	**intensity [cps] (5.0 mL H_2 min^{-1})**
16	$^{16}O^+$ $^1H_2{}^{14}N^+$	57 ± 6	8.9 ± 3.1	< CL
17	$^{16}O^1H^+$ $^1H_3{}^{14}N^+$	302 ± 19	6.5 ± 2.4	< CL
18	$^1H_2{}^{16}O^+$	125700 ± 800	7.2 ± 3.0	< CL
19	$^1H_3{}^{16}O^+$	1480 ± 40	522 ± 23	7.2 ± 3.1
20	$^1H_2{}^{18}O^+$	557 ± 22	10 ± 4	< CL
21	$^1H_3{}^{18}O^+$	37 ± 7	6.9 ± 2.5	< CL
23	$^{23}Na^+$	18 ± 5	5.7 ± 2.6	< CL
24	$^{24}Mg^+$	17.7 ± 3.4	< CL	< CL
25	$^{25}Mg^+$	15.8 ± 3.4	< CL	< CL
26	$^{26}Mg^+$ $^{12}C_2{}^1H_2{}^+$	33 ± 5	5.7 ± 2.2	< CL
27	$^{27}Al^+$ $^{12}C_2{}^1H_3{}^+$	100 ± 10	35 ± 7	27 ± 4
28	$^{28}Si^+$ $^{14}N_2{}^+$	122700 ± 1100	3260 ± 70	1180 ± 40
29	$^{29}Si^+$ $^{28}Si^1H^+$ $^{14}N^{15}N^+$ $^1H^{14}N_2{}^+$	2970 ± 60	6050 ± 80	439 ± 24
30	$^{30}Si^+$ $^{29}Si^1H^+$ $^{14}N^{16}O^+$ $^{15}N_2{}^+$	7620 ± 90	8460 ± 110	4460 ± 60
31	$^{15}N^{16}O^+$ $^{14}N^{16}O^1H^+$	161 ± 13	120 ± 10	67 ± 8
32	$^{32}S^+$ $^{16}O_2{}^+$	30630 ± 310	6840 ± 90	4010 ± 70
33	$^{33}S^+$ $^{16}O_2{}^1H^+$	900 ± 40	407 ± 21	52 ± 8
34	$^{34}S^+$ $^{16}O^{18}O^+$	222 ± 15	179 ± 13	60 ± 10
35	$^{35}Cl^+$	160 ± 10	16.4 ± 3.4	4.9 ± 1.8
36	$^{36}Ar^+$	178100 ± 1500	16.0 ± 2.8	< CL
37	$^{37}Cl^+$ $^{36}Ar^1H^+$	2210 ± 50	1260 ± 40	36 ± 6
38	$^{38}Ar^+$	9320 ± 120	45 ± 5	9.2 ± 2.2
39	$^{39}K^+$ $^{38}Ar^1H^+$	787 ± 22	19140 ± 110	11980 ± 140
40	$^{40}Ar^+$	317400 ± 2400	731 ± 30	264 ± 17
41	$^{41}K^+$ $^{40}Ar^1H^+$	3060 ± 60	507000 ± 4000	1320 ± 40
42	$^{40}Ar^1H_2{}^+$	1300 ± 29	2350 ± 40	23 ± 4
43		576 ± 23	850 ± 25	14.3 ± 3.2
44	$^{12}C^{16}O_2{}^+$	320 ± 14	331 ± 14	12.3 ± 2.9
45		190 ± 10	741 ± 21	120 ± 10
46		141 ± 11	119 ± 7	11.0 ± 3.2

Table A.1 continued from previous page

m/z	species	intensity [cps] (0 mL H_2 min^{-1})	intensity [cps] (2.5 mL H_2 min^{-1})	intensity [cps] (5.0 mL H_2 min^{-1})
47		125 ± 11	77 ± 6	11 ± 4
48		89 ± 7	50 ± 4	5.9 ± 2.3
49		69 ± 7	37 ± 5	< CL
50	$^{50}Cr^+$	72 ± 6	42 ± 7	12.8 ± 3.0
51		58 ± 9	26 ± 5	6.4 ± 2.8
52	$^{52}Cr^+$ $^{40}Ar^{12}C^+$	192 ±15	240 ± 14	167 ± 13
53	$^{53}Cr^+$ $^{40}Ar^{13}C^+$	51 ± 7	39 ± 6	24 ± 5
54	$^{54}Cr^+$ $^{40}Ar^{14}N^+$	4330 ± 60	421 ± 17	48 ± 6
55	$^{55}Mn^+$ $^{40}Ar^{15}N^+$	130 ± 9	114 ± 10	90 ± 8
56	$^{56}Fe^+$ $^{40}Ar^{16}O^+$	660 ± 25	392 ± 19	438 ± 15
57	$^{57}Fe^+$ $^{40}Ar^{16}O^1H^+$	47 ± 6	80 ± 8	54 ± 6
58	$^{58}Fe^+$ $^{58}Ni^+$	729 ± 22	1300 ± 40	600 ± 23
59		88 ± 10	140 ± 10	54 ± 7
60	$^{60}Ni^+$	295 ± 19	534 ± 23	238 ± 17
61	$^{61}Ni^+$	33 ± 6	34 ± 6	15.7 ± 3.2
62	$^{62}Ni^+$	61 ± 6	88 ± 9	40 ± 6
63	$^{63}Cu^+$ $^{40}Ar^{23}Na^+$	40 ± 6	7 ± 7	30 ± 6
64	$^{64}Ni^+$ $^{64}Zn^+$	38 ± 6	31 ± 5	15 ± 4
65	$^{65}Cu^+$	32 ± 4	33 ± 7	18 ± 4
66	$^{66}Zn^+$	30 ± 5	22 ± 4	8.9 ± 3.1
67	$^{67}Zn^+$	22 ± 4	11.5 ± 3.0	< CL
68	$^{68}Zn^+$	567 ± 22	16 ± 4	6.2 ± 2.6
69	$^{69}Ga^+$ $^{12}C_3{}^{16}O_2{}^1H^+$	69 ± 8	20 ± 5	7.8 ± 2.4
70	$^{70}Ge^+$ $^{70}Zn^+$	33 ± 5	20 ± 4	13 ± 4
71	$^{71}Ga^+$	17 ± 4	9.1 ± 2.8	< CL
72	$^{72}Ge^+$	50 ± 8	35 ± 7	21 ± 4
73	$^{73}Ge^+$	29 ± 5	24 ± 4	20 ± 4
74	$^{74}Ge^+$ $^{74}Se^+$	55 ± 5	35 ± 5	25 ± 5
75	$^{75}As^+$	37 ± 6	22 ± 5	12 ± 4
76	$^{40}Ar^{36}Ar^+$ $^{38}Ar_2{}^+$	2350 ± 60	12 ± 4	7.4 ± 2.8
77	$^{77}Se^+$ $^{40}Ar^{36}Ar^1H^+$ $^{38}Ar_2{}^1H^+$	64 ± 7	6.8 ± 2.6	< CL
78	$^{78}Se^+$ $^{78}Kr^+$ $^{40}Ar^{38}Ar^+$	553 ± 24	9.6 ± 3.3	< CL
79	$^{79}Br^+$ $^{40}Ar^{38}Ar^1H^+$	349 ± 17	57 ± 5	39 ± 6
80	$^{80}Kr^+$ $^{80}Se^+$ $^{40}Ar_2{}^+$	410800 ± 2700	33 ± 5	< CL
81	$^{81}Br^+$ $^{40}Ar_2{}^1H^+$	1590 ± 40	83 ± 9	47 ± 5
82	$^{82}Kr^+$ $^{82}Se^+$	884 ± 24	7.9 ± 2.1	< CL
83	$^{83}Kr^+$	495 ± 14	17 ± 4	< CL
84	$^{84}Kr^+$	584 ± 27	17.6 ± 2.7	< CL
85	$^{85}Rb^+$	190 ± 10	130 ± 10	48 ± 6
86	$^{86}Kr^+$	212 ± 13	< CL	< CL
87	$^{87}Rb^+$	78 ± 6	42 ± 7	17 ± 4
90	$^{90}Zr^+$	36 ± 6	< CL	< CL
91	$^{91}Zr^+$ $^{12}C_7{}^1H_7{}^+$	31 ± 6	< CL	< CL
92	$^{92}Zr^+$	27 ± 4	< CL	< CL
93		26 ± 4	< CL	< CL
94		25 ± 4	< CL	< CL

Table A.1 continued from previous page

m/z	species	intensity [cps] (0 mL H_2 min^{-1})	intensity [cps] (2.5 mL H_2 min^{-1})	intensity [cps] (5.0 mL H_2 min^{-1})
95		20.8 ± 3.1	< CL	< CL
96		18.0 ± 3.3	< CL	< CL
97		18 ± 4	6.0 ± 2.4	< CL
98		15.4 ± 3.1	< CL	< CL
99		14.4 ± 2.8	< CL	< CL
100		18 ± 4	< CL	< CL
101		14.5 ± 3.3	< CL	< CL
102		12.0 ± 2.5	< CL	< CL
103		11.9 ± 2.4	< CL	< CL
104		12.2 ± 2.8	< CL	< CL
105		11.2 ± 2.7	< CL	< CL
106		10.8 ± 3.3	< CL	< CL
107	$^{107}Ag^+$	15 ± 4	8.2 ± 2.6	5.7 ± 2.5
108		8.9 ± 2.3	< CL	< CL
109	$^{109}Ag^+$	16 ± 4	8.1 ± 2.7	< CL
110	$^{110}Cd^+$	12.2 ± 2.7	6.1 ± 2.5	< CL
111	$^{111}Cd^+$	14 ± 4	6.6 ± 2.1	< CL
112	$^{112}Cd^+$ $^{112}Sn^+$	19 ± 4	9.5 ± 3.1	5.9 ± 2.1
113	$^{113}Cd^+$	16 ± 4	6.0 ± 2.5	< CL
114	$^{114}Cd^+$	19 ± 4	13 ± 4	7.1 ± 1.6
115	$^{115}Sn^+$	8.5 ± 2.3	< CL	< CL
116	$^{116}Sn^+$ $^{116}Cd^+$	12.5 ± 3.1	5.7 ± 2.0	< CL
117	$^{117}Sn^+$	8.0 ± 2.3	< CL	< CL
118	$^{118}Sn^+$	8.6 ± 2.6	< CL	< CL
119	$^{119}Sn^+$	12.8 ± 3.3	< CL	< CL
120	$^{120}Sn^+$	10.2 ± 2.8	< CL	< CL
121	$^{121}Sb^+$	22 ± 4	12 ± 4	7.8 ± 3.0
123	$^{123}Sb^+$	16 ± 4	10.9 ± 2.9	7.5 ± 2.1
124	$^{124}Sn^+$ $^{124}Xe^+$	11 ± 4	< CL	< CL
125		8.0 ± 2.2	< CL	< CL
126	$^{126}Xe^+$	9.8 ± 3.0	< CL	< CL
127	$^{127}I^+$	213 ± 12	198 ± 11	115 ± 11
128	$^{128}Xe^+$	57 ± 7	52 ± 5	32 ± 5
129	$^{129}Xe^+$	662 ± 21	642 ± 18	365 ± 19
130	$^{130}Xe^+$	118 ± 9	106 ± 12	61 ± 7
131	$^{131}Xe^+$	580 ± 23	540 ± 27	311 ± 17
132	$^{132}Xe^+$	716 ± 23	700 ± 18	407 ± 23
133	$^{133}Cs^+$	27 ± 5	41 ± 5	28 ± 4
134	$^{134}Xe^+$	297 ± 22	284 ± 19	166 ± 11
135		9.2 ± 2.8	< CL	< CL
136	$^{136}Xe^+$	263 ± 14	245 ± 15	145 ± 7
141	$^{141}Pr^+$	9.2 ± 2.7	< CL	< CL
181		34 ± 8	< CL	< CL
197	$^{197}Au^+$	10 ± 4	6.1 ± 2.4	< CL
199	$^{199}Hg^+$	8.8 ± 2.3	< CL	< CL
200	$^{200}Hg^+$	9.8 ± 2.3	7.7 ± 1.8	6.3 ± 1.8
202	$^{202}Hg^+$	12 ± 4	9.7 ± 2.2	7.5 ± 2.2
205	$^{205}Tl^+$	13 ± 4	10.0 ± 2.0	10.5 ± 3.1
209	$^{209}Bi^+$	15 ± 4	9.8 ± 3.1	8.7 ± 3.3
220	BKG	2.4 ± 1.3	0.7 ± 0.7	0.3 ± 0.5
231		9 ± 4	< CL	< CL

References

(1) K. P. Jochum and U. Nohl, *Chemical Geology*, 2008, **253**, 50–53.